Macroscopic random Paschen-Back effect in ultracold atomic gases

M. Modugno,[1,2] E. Ya. Sherman,[3,2] and V. V. Konotop[4]
[1]*Department of Theoretical Physics and History of Science, University of the Basque Country UPV/EHU, 48080 Bilbao, Spain*
[2]*IKERBASQUE Basque Foundation for Science, Bilbao, Spain*
[3]*Department of Physical Chemistry, University of the Basque Country UPV/EHU, 48080 Bilbao, Spain*
[4]*Centro de Física Teórica e Computacional and Departamento de Física, Faculdade de Ciências, Universidade de Lisboa, Campo Grande 2, Edifício C8, Lisboa 1749-016, Portugal*
(Received 4 March 2017; published 23 June 2017)

We consider spin- and density-related properties of single-particle states in a one-dimensional system with random spin-orbit coupling. We show that the presence of an additional Zeeman field Δ induces both nonlinear spin polarization and delocalization of states localized at $\Delta = 0$, corresponding to a random macroscopic analog of the Paschen-Back effect. While the conventional Paschen-Back effect corresponds to a saturated Δ dependence of the spin polarization, here the gradual suppression of the spin-orbit coupling effects by the Zeeman field is responsible both for the spin saturation and delocalization of the particles.

DOI: 10.1103/PhysRevA.95.063620

I. INTRODUCTION

Spin and mass dynamics caused by spin-orbit coupling (SOC) constitute one of the most important and interesting topics in modern solid-state and condensed-matter physics [1–3]. Recent experiments with ultracold atomic gases have greatly extended the frontiers of this field, by realizing tunable artificial SOC, as well Zeeman fields, for Bose-Einstein condensates [4] and Fermi gases [5,6]. The possibility of studying the effects of strong SOC both experimentally and theoretically has revealed a rich phenomenology of these systems (see, e.g., Refs. [7–11]). In one-dimensional settings this phenomenology has been enhanced by the presence of additional potentials, such as lattices [12–14] or artificial defects in the SOC [15].

A key topic in low-dimensional solid state [16,17] and cold atomic [18–21] systems is the localization of particles by disorder. In the presence of SOC, the localization was studied in Ref. [22] and in a quasiperiodic potential in Ref. [23], where a mobility edge was observed. Short-term spin and density dynamics were considered in Ref. [24]. Yet another type of SOC—the random one—is naturally present in solids [25–27]. It can also be designed in cold atomic matter by randomizing the field producing the SOC.

The combined effect of spin-independent disorder and random SOC on the localization in two-dimensional lattices has been studied in Refs. [28,29] and the orbital effect of the magnetic field in these systems was addressed in Ref. [30]. In this paper we consider a continuous one-dimensional system with randomness solely in the SOC realization, and investigate the effect of the Zeeman field on the particle spins and localization. We show that similar to the conventional random potentials, SOC can lead to localization, here strongly dependent on the Zeeman field. In particular, we show that as the Zeeman splitting increases, the spin expectation values change strongly and, more importantly, the fraction of the localized states rapidly decreases. This offers the ability to localize or delocalize the states solely by acting at the particle spin. The weakening of the SOC effects in sufficiently strong Zeeman fields is known in atomic physics as the Paschen-Back (alias nonlinear Zeeman) effect [31–33]. Here we study the appearance of the Paschen-Back effect in a random macroscopic system, where, along with the spin dependence, the SOC effective weakening manifests itself as the delocalization of the states under increasing Zeeman splitting.

This paper is organized as follows. In Sec. II we introduce the random SOC field and present its main characteristics. In Sec. III we describe a general picture of the macroscopic random Paschen-Back effect. In Sec. IV this approach will be applied to the ground state of the system. Section V provides conclusions and outlook for future research. Some details of calculations and additional information are given in the Appendixes.

II. HAMILTONIAN, RANDOM FIELDS, AND THEIR CORRELATORS

We consider a system described by the following Hamiltonian with a spatially random SOC $\alpha(x)$:

$$H_0 = \frac{k^2}{2} + \frac{1}{2}[\alpha(x)k + k\alpha(x)]\sigma_z + \Delta\sigma_x, \tag{1}$$

where $k = -i\partial/\partial x$, 2Δ is the Zeeman splitting, and $\sigma_{x,z}$ are the Pauli matrices [34]. We use units $\hbar \equiv 1$ and particle mass $\equiv 1$, so that from now on all the quantities are expressed in dimensionless units. Since our results will be based on the probability and the spin density distributions, they are independent of the Zeeman field direction, provided that it is orthogonal to the z axis.

To emphasize the physical mechanism of the delocalization in the Paschen-Back effect, we use unitary transformation [35] $H_{\rm tr} = S^{-1}H_0S$ with $S = \exp[-iA(x)\sigma_z]$ to reduce the Hamiltonian to the form

$$H_{\rm tr} = \frac{k^2}{2} - \frac{1}{2}\alpha^2(x) + \Delta[\sigma_x \cos 2A(x) - \sigma_y \sin 2A(x)], \tag{2}$$

where

$$A(x) \equiv \int_{-L}^{x} \alpha(x')dx', \tag{3}$$

as we study a system of size $2L$, with $x \in [-L, L]$ [36].

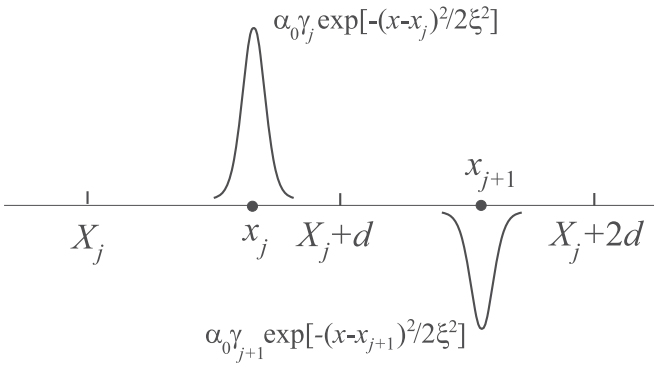

FIG. 1. Model distribution of SOC impurities corresponding to the disorder in Eq. (4).

At $\Delta = 0$, the Hamiltonian (2) describes two decoupled spin components in the random potential $-\alpha^2(x)/2$. The case of not random $\alpha(x)$ has been studied in Refs. [37–39]. The Zeeman coupling in Eq. (2) gives rise to an effective magnetic field which has a constant amplitude Δ and randomly varying direction: $\mathbf{m}(x) = (\cos 2A(x), -\sin 2A(x), 0)$.

As a model of disorder we consider the following:

$$\alpha(x) = \alpha_0 \sum_{j=1}^{N} \gamma_j e^{-(x-x_j)^2/2\xi^2}. \tag{4}$$

Here $j = 1, \ldots, N$ labels N "impurities" having equal widths ξ and located at points $x_j = X_j + d(r_j + 1/2)$, where $X_j \equiv -L + d(j-1)$, the impurity concentration is $1/d$, where $d = 2L/N$, and $\alpha_0\gamma_j$ are their strengths, as shown in Fig. 1. The statistics is described by independent uniform random distributions of γ_j and r_j, both in the range $[-0.5, 0.5]$. The resulting potential is bounded, $\alpha^2(x) \leqslant \alpha^2_{\max}$, and resembles optical speckles [40].

At $L \gg \max(\xi, d)$, the random SOC is characterized by two main parameters. The first one is the mean square $\langle\langle\alpha^2\rangle\rangle$, where $\langle\langle\ldots\rangle\rangle$ stands for the statistical averaging with the distributions of r_j and γ_j. The second parameter is the correlation length l_α of $\alpha(x)$. In the model of Eq. (4), $\langle\langle\alpha^2\rangle\rangle = \sqrt{\pi}\alpha_0^2\xi/12\,d$ and $l_\alpha = \sqrt{\pi}\xi$, as can be proven by straightforward calculations (e.g., by integration of the corresponding range function [26,27]).

To describe the spatial scale of the random Zeeman field, we introduce the correlator $\mathcal{K}_{mm}(x,x') \equiv \langle\langle \mathbf{m}(x)\mathbf{m}(x')\rangle\rangle$ and define the characteristic length $l_\mathbf{m}$ on which the direction $\mathbf{m}(x)$ varies significantly. This is the distance at which the correlation between $\mathbf{m}(x)$ and $\mathbf{m}(x + l_\mathbf{m})$ becomes weak, that is $|\mathcal{K}_{mm}(x,x')| \ll 1$ for $|x - x'| \gg l_\mathbf{m}$. The respective calculations can be done by taking into account that $A(x)$ is a random walk [41] in the $(x, A(x))$ space with small uncorrelated "steps" of the order of $\langle\langle\alpha^2\rangle\rangle^{1/2} l_\alpha \ll 1$ at the length scale of l_α. In this way we obtain (see Appendix A)

$$l_\mathbf{m} = \frac{1}{4\langle\langle\alpha^2\rangle\rangle l_\alpha}. \tag{5}$$

III. ZEEMAN FIELD DEPENDENCE: A GENERAL PICTURE

For $\Delta \neq 0$ the eigenstates of the Hamiltonian (1) are nondegenerate (except for accidental events). Such states are characterized by spinors $\boldsymbol{\psi}_n(x) = [\psi_{n1}(x), \psi_{n2}(x)]^{\mathrm{T}}$, where the number $n = 0, 1, \ldots$ labels their energies E_n. The spatial extension of state n is characterized by the inverse participation ratio (IPR) [42]:

$$\zeta_n = \int_{-L}^{L} [|\psi_{n1}(x)|^2 + |\psi_{n2}(x)|^2]^2 dx. \tag{6}$$

The symmetry of the Hamiltonian (1) implies that the only nonzero mean spin component is given by

$$\langle\sigma_x\rangle_n = 2\mathrm{Re}\int_{-L}^{L} \psi^*_{n1}(x)\psi_{n2}(x)dx. \tag{7}$$

Note that the eigenfunctions of (1) and (2) are mixed states in the spin subspace resulting in $\langle\sigma_x\rangle_n^2 \leqslant 1$ with $\langle\sigma_x\rangle_n^2 = 1$ for a pure and $\langle\sigma_x\rangle_n^2 = 0$ for the maximally mixed state, respectively.

Figure 2 presents the spin (a) and the IPR (b) as a function of n, for a single realization of the random potential, which is shown in Fig. 2(c). In Fig. 2(a) we observe that at small Δ most of the states are strongly mixed in spin subspace with $|\langle\sigma_x\rangle_n| \ll 1$. By increasing Δ, high-purity states appear at energies close to $\pm\Delta$ with $\langle\sigma_x\rangle_n$ increasing from approximately -1 to 1 with the energy increase from $-\Delta$ to Δ. The IPR of well-localized states, namely those with $\zeta_n \gtrsim 0.7$, strongly varies as a function of the state number [43] and reaches the disorder-free value $\zeta_L = 3/4L$ at sufficiently large n. For nonzero Δ, the n dependence of the IPR becomes more narrow, corresponding to the delocalization.

Figure 3 shows the disorder-averaged spin (a), the IPR (b), and the density of states (c) as a function of the energy. The IPR shows an *effective* mobility edge [44], which sharpens and shifts approximately to $-\Delta$ as Δ increases. As shown in the panel (c), at $\Delta = 0$ one observes a strong low-energy tail in the density of localized states. By increasing Δ, the number of the states in the tail decreases, demonstrating the delocalization, as clearly seen also in the inset of the panel (b).

To understand qualitatively the effect of the Zeeman field on delocalization, let us denote by l_s the distance that a particle can travel under the influence of the random magnetic field before its spin becomes uncorrelated with the initial one. By using again the random-walk approach, now in the coordinate-spin space, for a semiclassical particle moving with the velocity v, we obtain that l_s is determined by the condition $\Delta^2(l_\mathbf{m}/v)^2 l_s/l_\mathbf{m} \sim 1$, so that it is natural to define

$$l_s \equiv \frac{v^2}{\Delta^2 l_\mathbf{m}} = 4\frac{v^2\langle\langle\alpha^2\rangle\rangle l_\alpha}{\Delta^2}, \tag{8}$$

where $l_\mathbf{m}$ is given by Eq. (5). For states with energies E_n close to zero such that $|E_n| \ll \langle\langle\alpha^2\rangle\rangle$, we can make a semiclassical estimate $v^2 \sim \langle\langle\alpha^2\rangle\rangle$ and obtain $l_s \sim \langle\langle\alpha^2\rangle\rangle^2 l_\alpha/\Delta^2$.

Because long-range localization with $\zeta_n \ll l_\alpha$ occurs as a result of interference of waves with the same spin scattered by disorder [16,17], these localized states should have the characteristic length $1/\zeta_n \lesssim l_s$. Thus the random Zeeman field can destroy the localization [45]. On qualitative level, the destructive effect of decrease in l_s with Δ is seen in Figs. 2(b) and 3(b). Here, the states with $\zeta_n \gtrsim l_s^{-1}$ are still localized, while the higher-energy states are already delocalized, leading

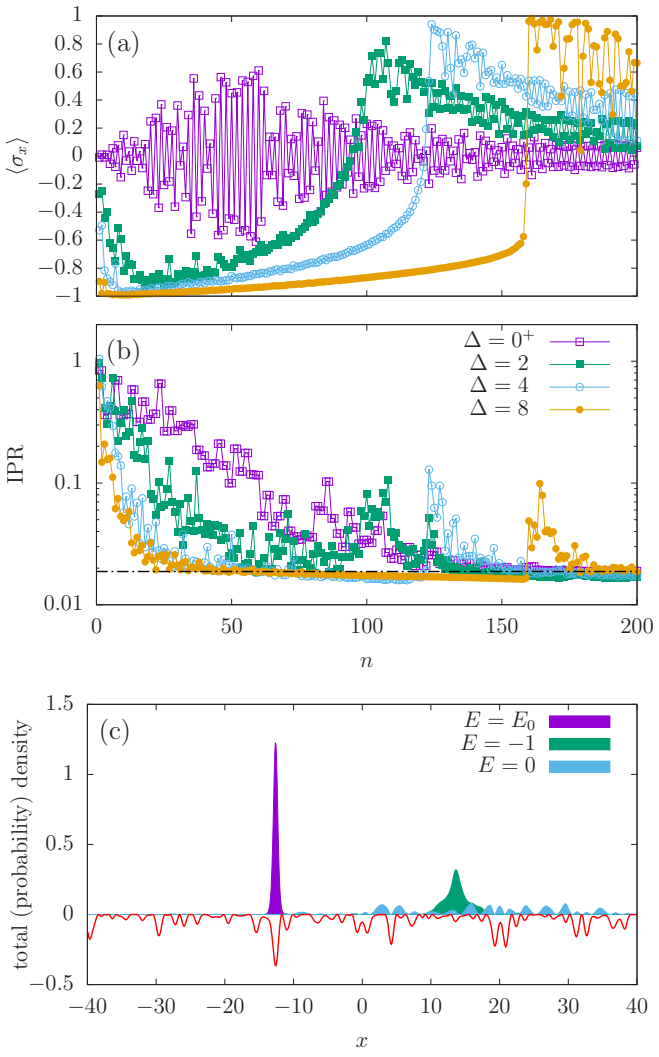

FIG. 2. (a) Spin component $\langle\sigma_x\rangle_n$ and (b) log scale of the IPR as a function of the state number for different Zeeman fields [the legend is shown in (b)]. To avoid degeneracy, we use here $0^+ = 10^{-3}$. The horizontal dash-dotted line corresponds to $\zeta_L = 3/4L$ value. (c) Actual realization of the random potential (solid line) and three densities corresponding to the energies $E_n = E_0, -1$, and 0. Here $\alpha_0 = 4$, $d = \xi = 0.5$, and $L = 40$.

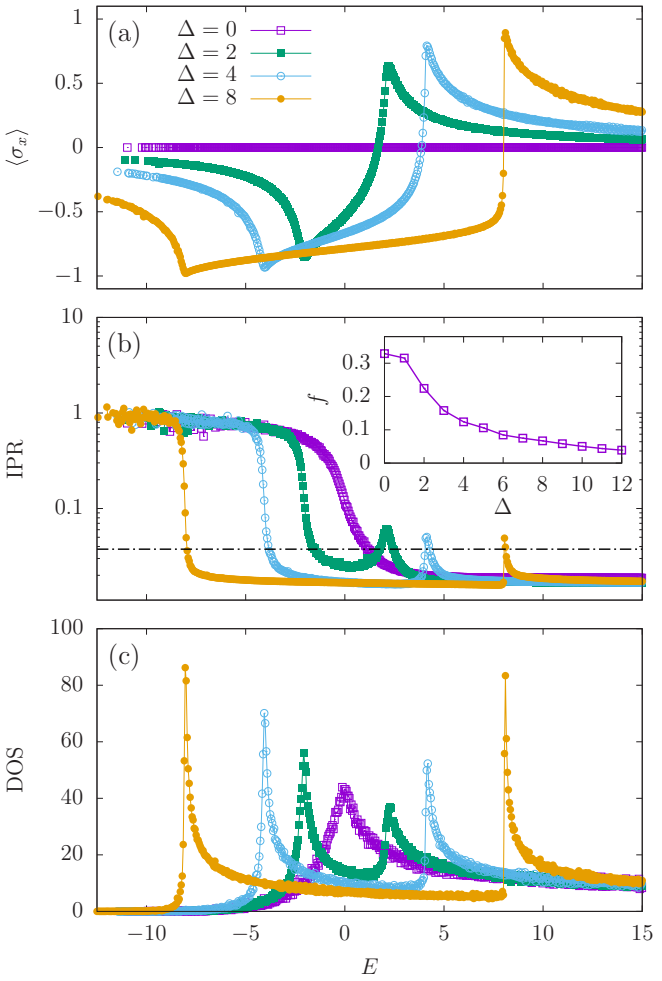

FIG. 3. Disorder-averaged quantities as a function of the state energy for different Zeeman Δ's [the legend is shown in (a)]. (a) Expectation value $\langle\sigma_x\rangle_n$, (b) the IPR, where the inset shows the fraction f of localized states (out of 300 lowest eigenstates) with the $\zeta_n > 2\zeta_L$ (dash-dot horizontal line), and (c) the density of states. The averaging is performed over $10^3\alpha(x)$ realizations with the parameters same as in Fig. 2.

to the observed sharpening of the effective mobility edge and shifting it to lower energies.

Since Hamiltonian (1) depends on spin randomly, in addition to the above argument based on comparison of the scales of ζ_n^{-1} and l_s, the delocalization and the dependence of $\langle\sigma_x\rangle_n$ on Δ can be obtained as follows. Let us consider the matrix form $\mathcal{H}_{pq}$ of Hamiltonian (1) in the representation of the degenerate basis states at $\Delta = 0$ defined as

$$\tilde{\boldsymbol{\psi}}_{2m} \equiv \begin{bmatrix} \phi_m(x) \\ 0 \end{bmatrix} e^{-iA(x)}, \quad \tilde{\boldsymbol{\psi}}_{2m+1} \equiv \begin{bmatrix} 0 \\ \phi_m(x) \end{bmatrix} e^{iA(x)}, \quad (9)$$

where $\phi_m(x)$ $(m = 0, 1, \ldots)$ are the real eigenfunctions with $\phi_m''(x) = -[\alpha^2(x) + 2\epsilon_m]\phi_m(x)$, and eigenenergies ϵ_m. In this basis the diagonal components are $\mathcal{H}_{2m,2m} = \mathcal{H}_{2m+1,2m+1} = \epsilon_m$ and the off-diagonal ones are expressed as

$$\mathcal{H}^*_{2m+1,2l} = \mathcal{H}_{2m,2l+1} \equiv \Delta \int_{-L}^{L} \phi_m(x)\phi_l(x)e^{2iA(x)}dx. \quad (10)$$

A broad Fourier spectrum of random $A(x)$ leads to appreciable transition coefficients $\mathcal{H}_{pq}/\Delta$ for localized states, which would be negligibly small otherwise even if such states have a considerable spatial overlap. This possibility of particle transfer between different states leads to delocalization at sufficiently strong Δ.

Now we can consider strong Zeeman field in more detail by addressing the source of suppression of the spin-conserving backscattering with the increase in Δ. At sufficiently large Δ, neglecting the SOC, the single particle states can be presented as $|k, \langle\sigma_x\rangle\rangle$, with $\langle\sigma_x\rangle = \pm 1$, corresponding to the eigenstates of σ_x in Eq. (1), momentum k, and energy $k^2/2 + \langle\sigma_x\rangle\Delta$. We consider the random SOC as a perturbation, which, however, prohibits the spin-conserving backscattering as the first-order

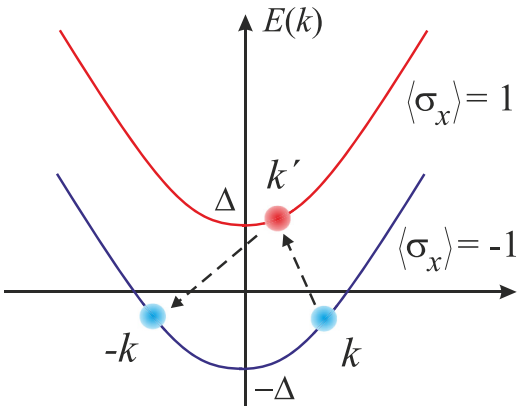

FIG. 4. Schematic illustration of the spin-conserving backscattering caused by the random SOC. Lower and upper parabolas correspond to $k^2/2-\Delta$ and $k^2/2+\Delta$ branches, respectively, with the virtual transitions shown by dashed lines.

process. Here this scattering $|k,-1\rangle \to |-k,-1\rangle$ occurs only by involving intermediate $|k',1\rangle$ states with the opposite spin, as schematically illustrated in Fig. 4. The corresponding spin-conserving backscattering matrix element behaves for $k^2 \ll 4\Delta$ as $\sim 1/\Delta$, strongly decreasing the scattering probability for low-energy states (see Appendix B) with the increase in Δ and thus leading to the delocalization.

IV. GROUND-STATE DEPENDENCE ON THE ZEEMAN FIELD

Now we consider how the developed approach can be applied to the properties of the ground state. According to the Hellmann-Feynman theorem [46], the expectation value of the spin of the ground state can be written as $\langle\sigma_x(\Delta=0)\rangle_0 = (dE_0/d\Delta)_{\Delta=0}$ and, therefore, obtained by the Δ-perturbation theory for the ground-state energy.

We begin by assuming that the Zeeman field is sufficiently weak such that the ground-state spin can be written as $\langle\sigma_x(\Delta)\rangle_0 = \langle\sigma_x(0)\rangle_0 + \Delta\, d\langle\sigma_x(\Delta)\rangle_0/d\Delta$, where the derivative is calculated at $\Delta=0$. Here the spin-split ground state forms a doublet well separated from the rest of the states. By using perturbation theory for degenerate states [32] in the basis of Eq. (9) we obtain the ground state:

$$\boldsymbol{\psi}_0(x) = \frac{1}{\sqrt{2}}\phi_0(x)\begin{bmatrix}\exp\left[-i(A(x)-\chi_0/2)\right]\\ -\exp\left[i(A(x)-\chi_0/2)\right]\end{bmatrix}, \tag{11}$$

where the phase χ_0 is defined by $\mathcal{H}_{01} \equiv |\mathcal{H}_{01}|\exp(i\chi_0)$. The condition of this weak-field approximation is $\max\left[|\mathcal{H}_{0,2m+1}|/(\epsilon_m-\epsilon_0)\right] \ll 1$ for $m \geqslant 1$.

To find $\langle\sigma_x(0)\rangle_0$, we assume that the ground-state wave function is localized near a point x_0 and can be approximated by a Gaussian of width l_0 as $\phi_0^2(x) \approx \exp\left[-(x-x_0)^2/l_0^2\right]/\pi^{1/2}l_0$. Next, by using $\boldsymbol{\psi}_0(x)$ in Eq. (11) and approximating $A(x) \approx A(x_0)+\alpha(x_0)(x-x_0)$ we obtain by Eq. (7):

$$\langle\sigma_x(0)\rangle_0 = -\exp\left[-\alpha^2(x_0)l_0^2\right]. \tag{12}$$

This value, being exponentially dependent on the ground-state parameters, strongly varies from realization to realization (see

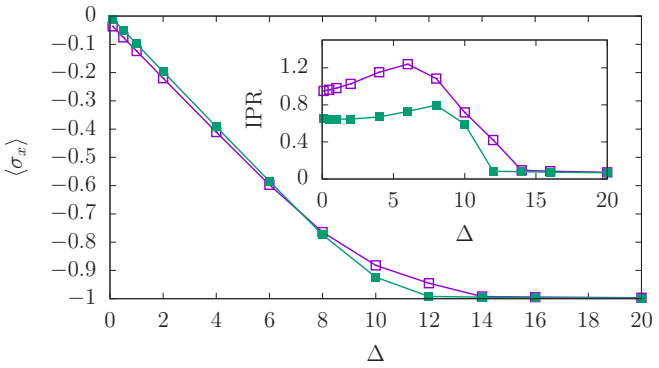

FIG. 5. Dependence of the ground state $\langle\sigma_x(\Delta)\rangle_0$ (main plot) and the IPR (inset) for two typical realizations of the random potential (see Appendix C for more details). As expected for low purity spin states, $|\langle\sigma_x(0)\rangle_0| \ll 1$, corresponding to typical $l_0|\alpha(x_0)| \geqslant 1$ for the chosen parameters of disorder, here the same as in Fig. 2.

Fig. 5). To get an order-of-magnitude estimate of $\langle\sigma_x(0)\rangle_0$ we consider a model ground state in the potential characterized by $\gamma_j = r_j = 0.5$ and $\gamma_{j+1} = -r_{j+1} = 0.5$. This state has the width $l_0 = \sqrt{\xi/\alpha_0}$ yielding $\langle\sigma_x(0)\rangle_0 = -\exp(-\alpha_0\xi)$. Next, we calculate the inverse participation ratio for this state as

$$\zeta_0(0) = \sqrt{\frac{\alpha_0}{2\pi\xi}}. \tag{13}$$

For given system parameters this yields $\zeta_0(0) \approx 1.12$, similar to the numerical results in the inset of Fig. 5.

Next, by means of the second-order perturbation theory and the Hellmann-Feynman theorem, one can obtain the linear in Δ term in $\langle\sigma_x(\Delta)\rangle_0$. To this end, we calculate Δ^2 correction to the energy by summing up over all transitions to the higher-energy states in the Eq. (9) basis. The maximal contribution to the energy correction is achieved at the states with energies $2\alpha^2(x_0)$, lying high above the effective mobility edge. Such states can be accurately approximated as $\sin(kx+\delta)/\sqrt{L}$, extended to the total length of the system with a slowly varying phase δ. The energy calculation can be done analytically by using the steepest descent method [47] [provided that $2\alpha(x_0)\,l_0 \gg 1$] resulting in

$$\frac{d\langle\sigma_x(\Delta)\rangle_0}{d\Delta} = -\frac{2}{|\epsilon_0|+2\alpha^2(x_0)}. \tag{14}$$

This value is less sensitive to the disorder realization than $\langle\sigma_x(0)\rangle_0$, as can be seen from the slope of $\langle\sigma_x(\Delta)\rangle_0$ in Fig. 5, presenting the numerical evidence for the random Paschen-Back effect. As it is seen in the main plot, $\langle\sigma_x(\Delta)\rangle_0$ tends to -1 at sufficiently large Δ, as expected for the conventional Paschen-Back effect [31]. Note that even at rather small Δ, the linear term greatly exceeds $\langle\sigma_x(0)\rangle_0$. The IPR shown in the inset initially increases (see the Appendixes), corresponding to a stronger localization, and then decreases to the values $\sim\zeta_L$, demonstrating the delocalization.

V. CONCLUSIONS AND OUTLOOK

We have studied the dependence of single-particle states on the Zeeman field in a one-dimensional system with random spin-orbit coupling. The observed dependence of the spin

is nonlinear with the saturation at a sufficiently strong field, corresponding to a macroscopic random Paschen-Back effect. In such a system, the spin saturation is accompanied by particle delocalization as both effects are due to suppression of the role of the random spin-orbit coupling. These effects could be engineered in a broad range of parameters in experimental setups for cold atomic gases, therefore permitting a variety of studies of this fundamental quantum effect at a macroscopic level. Although the calculated quantities are based on a particular model of disorder, our main estimates and qualitative results, being obtained by means of general arguments, are not restricted to the chosen model.

ACKNOWLEDGMENTS

M.M. and E.Y.S. acknowledge support by the Spanish Ministry of Economy, Industry and Competitiveness and the European Regional Development Fund FEDER through Grant No. FIS2015-67161-P (MINECO/FEDER, UE), and the Basque Government through Grant No. IT986-16. V.V.K. acknowledges support of the FCT (Portugal) under Grant No. UID/FIS/00618/2013. E.Y.S. is grateful to V. K. Dugaev and M. M. Glazov for valuable discussions, and to the National Science Center in Poland (Grant No. DEC-2012/06/M/ST3/00042) for partial support.

APPENDIX A: CORRELATOR OF THE RANDOM MAGNETIC FIELD

We present the correlator of the directions of the random magnetic field $\mathcal{K}_{mm}(x',x) \equiv \langle\langle \mathbf{m}(x')\mathbf{m}(x)\rangle\rangle$ as

$$\mathcal{K}_{mm}(x',x) = \langle\langle \cos[2(A(x') - A(x))]\rangle\rangle = \mathrm{Re}\left\langle\left\langle \prod_j \exp\left[2i\int_{X_j}^{X_j+d} \alpha(y)dy\right]\right\rangle\right\rangle, \quad \text{(A1)}$$

using the product over single-impurity intervals $(X_j, X_j + d)$ (as shown in Fig. 1), located between points x' and x and note that the distribution in Eq. (4) allows one to separate calculations of products and averaging. Taking a single interval and assuming for simplicity $\xi \ll d$ with

$$J_j \equiv 2\int_{X_j}^{X_j+d} \alpha(y)dy = 2\sqrt{2\pi}\gamma_j\alpha_0\xi \quad \text{(A2)}$$

yields

$$e^{iJ_j} = \cos(2\sqrt{2\pi}\gamma_j\alpha_0\xi) + i\,\sin(2\sqrt{2\pi}\gamma_j\alpha_0\xi). \quad \text{(A3)}$$

Since in the model of disorder we are considering, the expectation value $\langle\gamma_j\rangle = 0$, one obtains $\langle\langle\sin(2\sqrt{2\pi}\gamma_j\alpha_0\xi)\rangle\rangle = 0$. Employing a "small change" approximation $\alpha_0\xi \ll 1$ we obtain

$$\langle\langle\cos(2\sqrt{2\pi}\gamma_j\alpha_0\xi)\rangle\rangle = 1 - 4\pi\langle\gamma_j^2\rangle(\alpha_0\xi)^2 + O((\alpha_0\xi)^4). \quad \text{(A4)}$$

Making γ_j averaging with $\langle\gamma_j^2\rangle = 1/12$ and taking into account that $\langle\langle\alpha^2\rangle\rangle = \sqrt{\pi}/12 \times \alpha_0^2\xi/d$ yields with the same accuracy

$$\langle\langle\cos(2\sqrt{2\pi}\gamma_j\alpha_0\xi)\rangle\rangle = 1 - 4\sqrt{\pi}\langle\langle\alpha^2\rangle\rangle\xi d. \quad \text{(A5)}$$

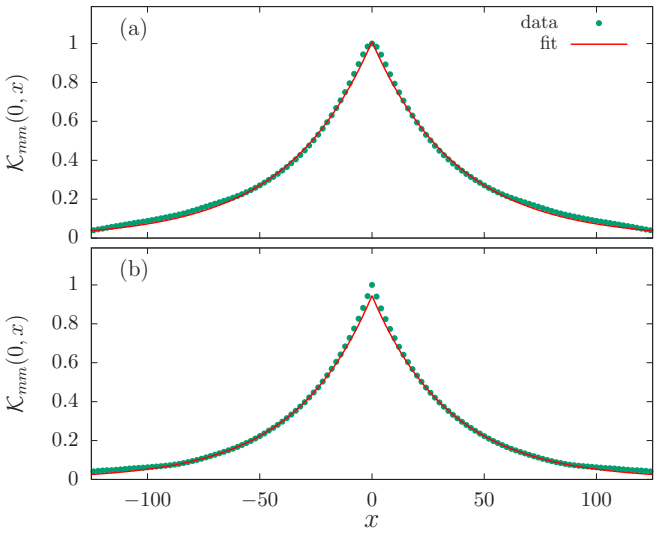

FIG. 6. Correlator $\mathcal{K}_{mm}(0,x)$ (averaged over 10^3 realizations) for two random potentials, both with $d = 0.5$. (a) $\alpha_0 = 1$, $\xi = d/4$, and best-fitting parameter $\beta = 0.03$; (b) $\alpha_0 = 0.06125$, $\xi = 4d$, and best-fitting parameter $\beta = 0.026$.

Next, we build the product over the intervals and obtain for $x' = 0$ and $d \ll |x| \ll L$ ($2L$ is the total system length)

$$\mathcal{K}_{mm}(0,x) = (1 - 4\sqrt{\pi}\langle\langle\alpha^2\rangle\rangle\xi d)^{|x|/d} \approx \exp(-\beta|x|), \quad \text{(A6)}$$

where $\beta = 4\sqrt{\pi}\langle\langle\alpha^2\rangle\rangle\xi$. The corresponding correlation length can be defined as

$$l_{\mathbf{m}} = \int_0^\infty \mathcal{K}_{mm}(0,x)dx = \frac{1}{4\sqrt{\pi}\langle\langle\alpha^2\rangle\rangle\xi}, \quad \text{(A7)}$$

where we put the upper integration limit to infinity and the lower limit to zero since we assume that $l_\alpha \ll l_{\mathbf{m}} \ll L$. By noting that in our model of disorder the correlation length of the spin-orbit coupling $l_\alpha = \sqrt{\pi}\xi$, we arrive at Eq. (5). While the coefficient $4\sqrt{\pi}$ in Eq. (A7) depends on the details of the model of disorder, the $l_{\mathbf{m}} \sim 1/\langle\langle\alpha^2\rangle\rangle\xi$ scaling is model independent. The numerical results are presented in Fig. 6 for two different sets of parameters. Note that at these values of α_0, ξ, and d one obtains $\beta \approx 0.033$ in agreement with the best fit of $\mathcal{K}_{mm}(0,x)$ (see caption of Fig. 6).

Having established the long-range behavior of the correlator, it would be of interest to obtain its short-distance behavior at $|x - x'| \ll l_\alpha$. Taking into account that at these short distances $A(x) - A(x') \approx \alpha(x)(x - x')$, we obtain after averaging of $\langle\langle\cos[2(A(x') - A(x))]\rangle\rangle$ in Eq. (A1)

$$\mathcal{K}_{mm}(x',x) = 1 - 2\langle\langle\alpha^2\rangle\rangle(x - x')^2. \quad \text{(A8)}$$

Note that short- and long-range behavior of $\mathcal{K}_{mm}(x,x')$ is due to different spatial scales. The long-range behavior is determined by $l_{\mathbf{m}}$ in Eq. (A7) while the short-range one (A8) is determined by the length $1/\langle\langle\alpha^2\rangle\rangle^{1/2}$. For the choice of parameters in Fig. 6 we have $l_{\mathbf{m}} \gg 1/\langle\langle\alpha^2\rangle\rangle^{1/2}$, leading to a cusplike dependence presented in this figure.

APPENDIX B: SPIN-CONSERVING BACKSCATTERING MATRIX ELEMENT: SPIN-ORBIT COUPLING AS A PERTURBATION

Here we illustrate the Δ dependence of the spin-conserving backscattering in the random spin-orbit coupling field and demonstrate that its probability rapidly decreases with the increase in Δ. We assume strong Zeeman field limit, which determines the spin states and the scattering due to the random spin-orbit coupling.

We consider spin-conserving transition $|k,\sigma_x=-1\rangle \to |-k,\sigma_x=-1\rangle$, which occurs at $k^2<4\Delta$ via virtual transitions to intermediate $|k',\sigma_x=1\rangle$ states, as shown in Fig. 4. Using second-order perturbation theory we obtain for the spin-conserving backscattering matrix element M_k resulting from interactions with random spin-orbit coupling impurities

$$M_k=\frac{1}{4}\int_{-\infty}^{\infty}\alpha_q\alpha_{2k+q}\frac{(2k+q)q}{2\Delta+(k+q)^2/2-k^2/2}\frac{dq}{2\pi}, \tag{B1}$$

where $q=k'-k$, and we have taken into account that the single spin-flip scattering matrix element between k and k' states is equal to $\alpha_{k'-k}(k+k')2$ [48], with the Fourier component

$$\alpha_p\equiv\int_{-\infty}^{\infty}\alpha(x)e^{-ipx}dx. \tag{B2}$$

The impurities have a Gaussian shape with the amplitude $|\gamma_j|=1$ resulting in $\alpha_p=\sqrt{2\pi}\alpha_0\xi\, e^{-p^2/2\xi^2}$ with $\alpha_q\alpha_{2k+q}=2\pi\alpha_0^2\xi^2e^{-[q^2+(2k+q)^2]\xi^2/2}$. Assuming a sufficiently large width ξ such that $\exp(-\Delta\xi^2)\ll 1$, we can use the steepest descent method to calculate the integral in Eq. (B1), where the maximum backscattering probability is due the "symmetric" transition with the momentum of the intermediate state $k+q=0$. As a result, we obtain for the matrix element for the states near the bottom of the $-\Delta$ subband

$$M_k=-\frac{\sqrt{\pi}}{8}\alpha_0^2\frac{\xi}{\Delta}k^2e^{-k^2\xi^2}. \tag{B3}$$

This value of $|M_k|^2$ rapidly decreases with the increase in Δ leading to delocalization by the Zeeman field.

APPENDIX C: Δ DEPENDENCE OF THE INVERSE PARTICIPATION RATIO

We begin with the study of the Δ dependence of the ground-state inverse participation ratio (IPR) in the limit of weak Zeeman field, where the analysis can be done perturbatively. We seek for the ground state $\tilde{\boldsymbol{\psi}}_0(x)$ in the form

$$\tilde{\boldsymbol{\psi}}_0(x)=\frac{\sqrt{1-\nu}}{\sqrt{2}}\begin{bmatrix}\psi_0(x)e^{i\chi_0/2}\\-\psi_0^*(x)e^{-i\chi_0/2}\end{bmatrix}+\frac{1}{\sqrt{2}}\sum_k\begin{bmatrix}p_k\psi_k(x)e^{i\chi_k/2}\\-p_k^*\psi_k^*(x)e^{-i\chi_k/2}\end{bmatrix}, \tag{C1}$$

where ψ_0 is the ground-state wave function in the $\Delta=0$ limit with the energy ϵ_0 [cf. Eq. (9)] and the functions $\psi_k(x)$ are extended over the system length $2L$ wave functions of the quasicontinuous spectrum with $\epsilon_k=k^2/2$. Small coefficients p_k can be obtained by perturbation theory as

$$p_k=\frac{\Delta}{\epsilon_k-\epsilon_0}\eta_k, \tag{C2}$$

where

$$\eta_k=e^{-i(\chi_0+\chi_k)/2}\int_{-L}^{L}\psi_0^*(x)\psi_k^*(x)dx. \tag{C3}$$

The parameter ν is a small probability to find the particle in a delocalized state:

$$\nu=\sum_k|p_k^2|=\frac{L}{\pi}\int_{-\infty}^{\infty}|p_k^2|dk, \tag{C4}$$

to conserve the total norm of the wave function. The probability ν can be calculated by the steepest descent method similarly to the second-order correction to the ground-state energy assuming the Gaussian ground state with the maximum probability density at x_0 point as

$$\nu=\frac{\Delta^2}{[|\epsilon_0|+2\alpha^2(x_0)]^2}. \tag{C5}$$

Function $|\tilde{\boldsymbol{\psi}}_0(x)|^4$ has a complex structure, with, however, only two terms giving finite contribution to the IPR in the $L\to\infty$ limit, as can be seen by counting the powers of L in the corresponding terms. The relevant contributions can be presented in the form:

$$|\tilde{\boldsymbol{\psi}}_0(x)|^4=(1-\nu)^2[|\psi_0(x)|^4+2|\psi_0(x)|^2\times(\psi_0^*(x)\psi_k(x)e^{-i\chi_0/2}e^{i\chi_k/2}p_k^*+\text{c.c.})]. \tag{C6}$$

Here we concentrate on these terms having different orders in Δ and present the inverse participation ratio in the form of the Δ expansion:

$$\zeta_0(\Delta)=\zeta_0(0)+\zeta_0'(0)\Delta+\tfrac{1}{2}\zeta_0''(0)\Delta^2. \tag{C7}$$

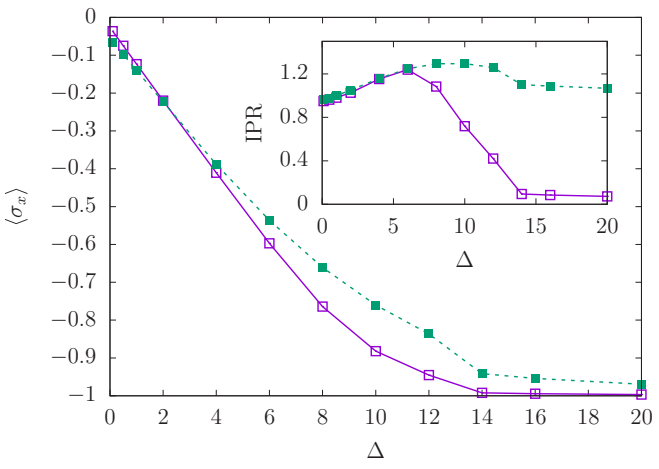

FIG. 7. Dependence of the ground-state spin on the Zeeman Δ for random (solid line) and regular [as in Eq. (C11), dashed line] SOC. These dependences are very similar for both types of coupling. Inset shows the qualitative difference between the IPR for the random and the regular realizations. While at small Δ the behavior of the IPR is the same, their large Δ dependences are different: the IPR rapidly decreases for the random SOC and returns to its value at $\Delta=0$ for the regular one.

By using Eq. (C6), the term quadratic in Δ can be rewritten as

$$\tfrac{1}{2}\zeta_0''(0)\Delta^2 = -2\zeta_0(0)\nu, \tag{C8}$$

leading to a decrease in $\zeta_0(\Delta)$ with the increase in the Zeeman field, as expected in the delocalization scenario.

The term linear in Δ has the form

$$\zeta_0'(0)\Delta = 2\sum_k \int_{-L}^{L} |\psi_0(x)|^2(\psi_0^*(x)\psi_k(x) \times e^{-i(\chi_0-\chi_k)/2}p_k^* + \text{c.c.})dx. \tag{C9}$$

Note that, while $\psi_0(x)$ and $\psi_k(x)$ are orthogonal, $|\psi_0(x)|^2\psi_0(x)$ and $\psi_k(x)$ are, in general, not. As a result we obtain the linear correction to the IPR in the form

$$\zeta_0'(0) = 4\,\mathrm{Re}\sum_k \frac{e^{-i\chi_0}}{\epsilon_k-\epsilon_0}\int_{-L}^{L}\psi_0^*(x)\psi_k^*(x)dx \times \int_{-L}^{L}|\psi_0(x)|^2\psi_0^*(x)\psi_k(x)dx, \tag{C10}$$

demonstrating that IPR can behave linearly with Δ, as presented in Fig. 7, due to change in the shape of the ground-state wave function by adding strongly x-dependent functions varying on the spatial scale less than the spatial scale of $\psi_0(x)$.

One more point on the importance of disorder deserves to be mentioned here. To demonstrate its role, we have chosen a realization of $\alpha(x)$ and performed a calculation of the Δ-dependent IPR of the ground state with the Hamiltonian

$$H = \frac{k^2}{2} + V(x) + \alpha(x_0)k\sigma_z + \Delta\sigma_z, \tag{C11}$$

where $V(x) = -\alpha^2(x)/2$ and x_0 is the position of the maximum of the ground-state density in this potential. Note that Hamiltonian (C11) resembles the Hamiltonian (1), but has a constant SOC. At sufficiently small Δ the properties of the ground state are determined mostly by local SOC $\alpha(x_0)$. The effect of the randomness becomes visible only at relatively large Δ, where the ground state is already modified by a contribution of the extended states. Although in both cases the value of spin saturates at $\langle\sigma_x\rangle = -1$, as expected in the conventional Paschen-Back effect, the localization is restored for a constant SOC and disappears for a random one, as can be seen in Fig. 7. This is due to different properties of the interstate transition matrix elements [see Eq. (10)], where the broad Fourier spectrum of random $A(x)$ extends the set of transitions while for a regular coupling this set is strongly restricted and delocalization does not occur.

[1] *Spin Physics in Semiconductors*, Springer Series in Solid-State Sciences, edited by M. I. Dyakonov (Springer, New York, 2008).

[2] T. D. Stanescu, B. Anderson, and V. Galitski, Phys. Rev. A **78**, 023616 (2008); V. Galitski and I. B. Spielman, Nature (London) **494**, 49 (2013).

[3] H. Zhai, Int. J. Mod. Phys. B **26**, 1230001 (2012).

[4] Y.-J. Lin, K. Jiménez-García, and I. B. Spielman, Nature (London) **471**, 83 (2011).

[5] P. Wang, Z.-Q. Yu, Z. Fu, J. Miao, L. Huang, S. Chai, H. Zhai, and J. Zhang, Phys. Rev. Lett. **109**, 095301 (2012).

[6] L. W. Cheuk, A. T. Sommer, Z. Hadzibabic, T. Yefsah, W. S. Bakr, and M. W. Zwierlein, Phys. Rev. Lett. **109**, 095302 (2012).

[7] J.-Y. Zhang, S.-C. Ji, Z. Chen, L. Zhang, Z.-D. Du, B. Yan, G.-S. Pan, B. Zhao, Y.-J. Deng, H. Zhai, S. Chen, and J.-W. Pan, Phys. Rev. Lett. **109**, 115301 (2012).

[8] Ch. Qu, Ch. Hamner, M. Gong, Ch. Zhang, and P. Engels, Phys. Rev. A **88**, 021604 (2013).

[9] G. I. Martone, Y. Li, L. P. Pitaevskii, and S. Stringari, Phys. Rev. A **86**, 063621 (2012).

[10] Y. Zhang, L. Mao, and Ch. Zhang, Phys. Rev. Lett. **108**, 035302 (2012).

[11] Q.-Q. Lü and D. E. Sheehy, Phys. Rev. A **88**, 043645 (2013).

[12] J. Larson, J.-P. Martikainen, A. Collin, and E. Sjöqvist, Phys. Rev. A **82**, 043620 (2010); Y. Zhang and C. Zhang, *ibid.* **87**, 023611 (2013); M. Salerno and F. Kh. Abdullaev, Phys. Lett. A **379**, 2252 (2015); M. Salerno, F. Kh. Abdullaev, A. Gammal, and L. Tomio, Phys. Rev. A **94**, 043602 (2016).

[13] Y. V. Kartashov, V. V. Konotop, D. A. Zezyulin, and L. Torner, Phys. Rev. Lett. **117**, 215301 (2016).

[14] Y. V. Kartashov, V. V. Konotop, and F. K. Abdullaev, Phys. Rev. Lett. **111**, 060402 (2013); V. E. Lobanov, Y. V. Kartashov, and V. V. Konotop, *ibid.* **112**, 180403 (2014).

[15] Y. V. Kartashov, V. V. Konotop, and D. A. Zezyulin, Phys. Rev. A **90**, 063621 (2014).

[16] P. W. Anderson, Phys. Rev. **109**, 1492 (1958).

[17] V. L. Berezinskii, Sov. Phys. JETP **38**, 620 (1974); L. P. Gor'kov, in *Electron-electron Interactions in Disordered Systems*, edited by A. L. Efros and M. Pollak (North-Holland, Amsterdam, 1985), p. 619.

[18] C. Skokos, D. O. Krimer, S. Komineas, and S. Flach, Phys. Rev. E **79**, 056211 (2009).

[19] A. S. Pikovsky and D. L. Shepelyansky, Phys. Rev. Lett. **100**, 094101 (2008).

[20] M. Larcher, F. Dalfovo, and M. Modugno, Phys. Rev. A **80**, 053606 (2009).

[21] I. L. Aleiner, B. L. Altshuler, and G. V. Shlyapnikov, Nat. Phys. **6**, 900 (2010).

[22] For one-dimensional systems, see L. Zhou, H. Pu, and W. Zhang, Phys. Rev. A **87**, 023625 (2013); for two-dimensional speckles: G. Orso, Phys. Rev. Lett. **118**, 105301 (2017).

[23] C. Li, F. Ye, Y. V. Kartashov, V. V. Konotop, and X. Chen, Sci. Rep. **6**, 31700 (2016).

[24] Sh. Mardonov, M. Modugno, and E. Ya. Sherman, Phys. Rev. Lett. **115**, 180402 (2015).

[25] M. M. Glazov, E. Ya. Sherman, and V. K. Dugaev, Physica E (Amsterdam) **42**, 2157 (2010).

[26] M. M. Glazov and E. Ya. Sherman, Phys. Rev. Lett. **107**, 156602 (2011).

[27] J. R. Bindel, M. Pezzotta, J. Ulrich, M. Liebmann, E. Y. Sherman, and M. Morgenstern, Nat. Phys. **12**, 920 (2016).

[28] S. N. Evangelou, Phys. Rev. Lett. **75**, 2550 (1995).

[29] Y. Asada, K. Slevin, and T. Ohtsuki, Phys. Rev. Lett. **89**, 256601 (2002).

[30] C. Wang, Y. Su, Y. Avishai, Y. Meir, and X. R. Wang, Phys. Rev. Lett. **114**, 096803 (2015).
[31] F. Paschen and E. Back, Ann. Phys. **344**, 897 (1912); **345**, 960 (1913).
[32] L. D. Landau and E. M. Lifshitz, *Quantum Mechanics* (Butterworth-Heinemann, Oxford, UK, 1981).
[33] B. H. Bransden and C. J. Joachain, *Physics of Atoms and Molecules* (Longman, New York, 1982).
[34] Note that, although the spatial motion is strictly one dimensional, spin-related features are fully three dimensional.
[35] L. S. Levitov and E. I. Rashba, Phys. Rev. B **67**, 115324 (2003).
[36] The size of the system should be sufficiently larger than the disorder-induced localization length in the energy interval of interest. A practical check for a length choice is based on comparing systems of size L, $2L$, and $4L$, verifying that finite-L effects and boundary conditions are not substantial.
[37] D. Sánchez and L. Serra, Phys. Rev. B **74**, 153313 (2006); D. Sánchez, L. Serra, and M.-S. Choi, *ibid.* **77**, 035315 (2008).
[38] M. Valín-Rodriguez, A. Puente, and L. Serra, Phys. Rev. B **69**, 085306 (2004).
[39] J. Cserti, A. Csordás, and U. Zülicke, Phys. Rev. B **70**, 233307 (2004).
[40] G. M. Falco, A. A. Fedorenko, J. Giacomelli, and M. Modugno, Phys. Rev. A **82**, 053405 (2010).
[41] J. R. Norris, *Markov Chains*, Cambridge Series on Statistical and Probabilistic Mathematics (Cambridge University Press, Cambridge, UK, 1998).
[42] In contrast to lattice models [20,28–30], in a continuous one-dimensional system, the IPR has units of inverse length being not limited by 1 from above. The IPR of the order of $1/2L$ corresponds to delocalized states in terms of the present model.
[43] F. Evers and A. D. Mirlin, Phys. Rev. Lett. **84**, 3690 (2000).
[44] The occurrence of an *effective* mobility edge is typical of speck-lelike potentials; see, e.g., L. Sanchez-Palencia, D. Clément, P. Lugan, P. Bouyer, G. V. Shlyapnikov, and A. Aspect, Phys. Rev. Lett. **98**, 210401 (2007); for special shapes of correlated potentials demonstrating the mobility edge, see F. M. Izrailev and A. A. Krokhin, *ibid.* **82**, 4062 (1999).
[45] S. Hikami, A. I. Larkin, and Y. Nagaoka, Prog. Theor. Phys. **63**, 707 (1980).
[46] R. P. Feynman, Phys. Rev. **56**, 340 (1939).
[47] J. Mathews and R. L. Walker, *Mathematical Methods of Physics* (W. A. Benjamin, Inc., New York, 1964).
[48] V. K. Dugaev, E. Ya. Sherman, V. I. Ivanov, and J. Barnaś, Phys. Rev. B **80**, 081301 (2009).